EPJ Web of Conferences will be set by the publisher
DOI: will be set by the publisher

News on Collectivity in PbPb Collisions at CMS

Dong Ho Moon[1,a] on behalf of the CMS Collaboration

[1] *Chonnam National University, 61186, Gwangju, Republic of Korea*

Abstract. The flow anisotropies with the Fourier coefficients (n = 2, 3) for the charged particles produced in PbPb collisions at a nucleon-nucleon center-of-mass energy of 5.02 TeV is studied with the CMS detector. In order to extract the Fourier coefficients, several methods were used, such as the scalar product method or multi-particle cumulant method. The results cover both of the low-p_T region ($1 < p_T < 3$ GeV/c) associated with hydrodynamic flow phenomena and the high-p_T region where anisotropic azimuthal distributions may reflect the path-length dependence of the parton energy loss in the created medium for the seven bins of collision centrality, spanning the rang of 0-60% most-central events.

1 Introduction

A Quark-Gluon-Plasma (QGP) is a state of matter which quantum chromodynamic (QCD) predicts that it will occur at extremely high temperature and density. The experiments at the Relativistic Heavy Ion Collider (RHIC) have established the formation of QGP in ultra-relativistic nucleus-nucleus interactions [1–4]. One of strong signatures of the existence for QGP is the suppression of high-transverse-momentum (p_T) hadron yield via the nuclear modification factor, R_{AA}, which is the ratio of the final-state particle yields at a given p_T value to that expected based on a scaling of pp collision results in the absence of the medium [1–4]. The observation of dijet asymmetry in PbPb collisions at the Large Hadron Collider (LHC) furnishes further proof of jet quenching, indicating a large energy loss for partons traversing the QGP medium.

The measurement of R_{AA} alone is not sufficient to differentiate among various parton energy-loss models. In addition, it has been shown that R_{AA} is not sensitive to sub-nucleon spatial fluctuations [5]. Additional observables, such as the azimuthal anisotropy of high p_T hadrons, are needed to constrain the models [6–12]. The anisotropy can be characterized by the coefficient of the second-order Fourier harmonic, v_2, in the azimuthal angle ϕ distribution of the hadron yield relative to the reaction-plane angle Ψ_{RP}, $dN/d\phi \propto 1 + 2v_2 \cos(2(\phi - \Psi_{RP}))$, where Ψ_{RP} is defined by the short-axis direction of the "almond"-shaped interaction region created in a non-central heavy-ion collision. In order to reduce the ambiguity on the measurement, scalar product or multi-particle cumulant methods can be replaced.

Furthermore, v_3, the coefficient of the higher harmonic, is particularly sensitive to the initial-state fluctuations. Indeed, v_3 arises mainly from fluctuation in the soft sector and it remains to be seen if these fluctuations can generate triangular anisotropy at high p_T.

In this paper, a study of the azimuthal anisotropy of very high p_T particles (up to $p_T \approx 100$GeV/c) for PbPb collisions at $\sqrt{s_{NN}} = 5.02$ TeV at the LHC using the CMS detector is presented. The v_2 and

[a] e-mail: dmoon@cern.ch

v_3 coefficients are determined as a function of p_T and collision centrality in the pseudorapidity regions of $|\eta| < 1$, where $\eta = -\ln[\tan(\theta/2)]$ and θ is the polar angle relative to the counterclockwise beam direction. The first precise measurement of the v_2 and v_3 coefficients up to very high p_T region in heavy-ion collisions are represented by using scalar product method and the multi-particle cumulant analysis for several orders (4, 6 and 8) as a function of p_T.

2 Experimental Setup

2.1 Event Selection

For this analysis, 2015 PbPb data at $\sqrt{s_{\rm NN}}$ = 5.02 TeV is utilized with an integrated luminosity of 404 μb^{-1}. Events were selected by using several trigger combinations in different p_T regions and centrality bins. The minimum-bias trigger covers the low p_T region (< 14 GeV/c), while the dedicated triggers on high p_T tracks are used for high p_T region up to 100 GeV/c. The L1 trigger seed of the triggers fired based on the highest ET Regional Calorimeter Trigger (RCT) region in the barrel of the CMS detector ($|\eta| < 1.0$). At the High Level Trigger (HLT), the leading track is passing the strict quality selection criteria describes in section 2.2. The performances of trigger for tracks used in analysis are shown in Figure 1.

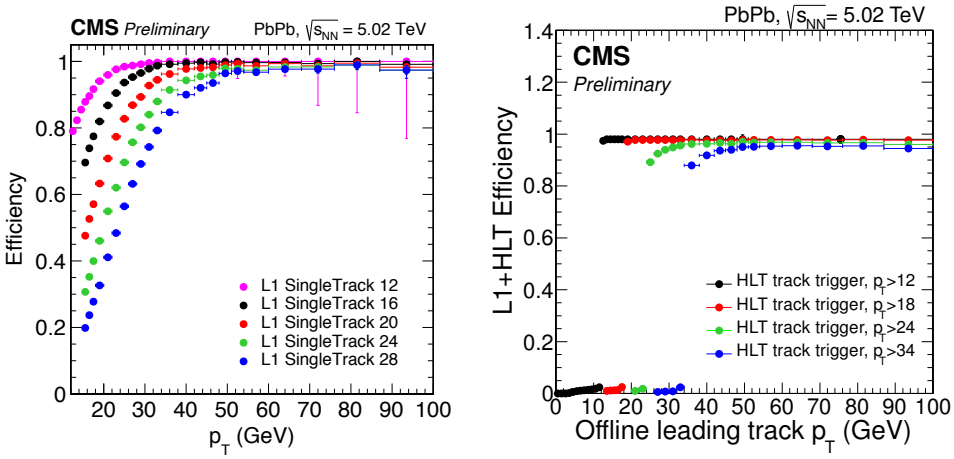

Figure 1. The efficiencies of L1 trigger (left) and High level trigger (right) as a function of p_T measured in $|\eta| < 1.0$. L1 trigger efficiencies are estimated for p_T of 12, 16, 20, 24 and 28 GeV/c, and HLT efficiencies are done in the p_T regions of 12, 18, 24 and 34 GeV/c [13].

2.2 Track Selection

Primary-track candidates are selected by the high-purity tracks. Additional requirements are also applied to enhance the purity of primary tracks. The significance of the separation along the beam axis (z) between the track and the best vertex, $dz/\sigma(dz)$, and the significance of the impact parameter relative to the best vertex transverse to the beam, $d_T/\sigma(d_T)$, should be less than 3. The relative uncertainty of the transverse-momentum measurement, $\sigma(p_T)/p_T$, must be less than 10%. In order to

reduce the fake rate of mis-reconstructed tracks and confirm high tracking efficiency, primary tracks with $|\eta| < 1.0$ and $p_T > 1.0$ GeV/c are used in the analysis. Furthermore, tracks above 20 GeV/c in the tracker are required to match with an energy deposit in the calorimeter to further decrease the fake rate.

3 Analysis Methods

3.1 Scalar product method

The "scalar-product" event-plane method is used to study azimuthal correlations with long-range of pseudorapidity. The event-plane is determined event-by-event and consists of the beam direction and the azimuthal direction of maximum particle density.

Avoiding autocorrelation effects where a given particle, or its decay products is very important to determine the event plane which we want to characterize. This is usually done by requiring a large gap in pseudorapidity between the particles used to establish the event plane and those used to determine the Fourrier coefficients.

The azimuthal dependence of the particle yield can be written in terms of an harmonic expansion with [14]

$$E\frac{d^3N}{d^3p} = \frac{1}{2\pi}\frac{d^2N}{p_T dp_T dy}\left(1 + \sum_{n=1}^{\infty} 2v_n \cos\left[n\left(\phi - \Psi\right)\right]\right) \tag{1}$$

where ϕ and E are the particle's azimuthal angle and energy, respectively. If the impact-parameter direction is known, the reference angle Ψ can be decided as the azimuthal angle of the reaction plane Ψ_R as defined by the beam and impact parameter directions.

To make the largest pseudorapidity gap possible, elliptic flow ($n = 2$) and triangular flow ($n = 3$) event planes are defined using calorimeter data, with the HF_n^- planes covering the pseudorapidity range of $-5 \leq \eta < -3$ and HF_n^+ planes covering the range $3 \leq \eta < 5$. Another event plane using tracker data with $-0.75 \leq \eta < 0.75$ was also defined and used in the three-sub-event technique for determining the resolution corrections for the HF_n^-, HF_n^+. To consider asymmetries that arise from the detector acceptance and other effects correlated with the detector conditions, a two-step process is used where the event plane is first recentered and subsequently flattened [15].

In order to measure the actual v_n coefficients, the current analysis utilizes the scalar product method introduced firstly by the STAR collaboration in a study of elliptic flow in AuAu collisions at $\sqrt{s_{\rm NN}} =$ 130 GeV [16]. The Q-vectors are defined as

$$Q_n \equiv \sum_{i=1}^{M} e^{in\phi_i}, \tag{2}$$

where M is the number of particles in each event. Therefore, using the scalar product method, v_n harmonics can be expressed as

$$v_n\,\{\mathrm{SP}\} \equiv \frac{\left\langle Q_n Q_{nA}^* \right\rangle}{\sqrt{\frac{\langle Q_{nA} Q_{nB}^* \rangle \langle Q_{nA} Q_{nC}^* \rangle}{\langle Q_{nB} Q_{nC}^* \rangle}}}. \tag{3}$$

Here, the subscripts A, B, and C refer to three separate event planes reconstructed in different regions of pseudorapidity. The particles of interest are expressed by the Q_n vector and are correlated with the A event plane. The event planes B and C effectively correct for the finite resolution of the A event plane that results from finite particle multiplicities and detector effects [17].

3.2 Multi-particle correlation technique with cumulants

Another way to measure v_2 is the Q-Cumulant method [18, 19] from 4-, 6- and 8-particle correlations. This method supplies a fast, exact (no approximations), and unbiased (no interference between different harmonics) estimations for the cumulants. The cumulants are expressed in terms of the moments of the magnitude of the Q_n flow vector. We first define the m-particle (m = 2, 4, 6 or 8) correlator as

$$\begin{aligned}
\langle\langle 2\rangle\rangle &\equiv \left\langle\left\langle e^{in(\phi_1-\phi_2)}\right\rangle\right\rangle \\
\langle\langle 4\rangle\rangle &\equiv \left\langle\left\langle e^{in(\phi_1+\phi_2-\phi_3-\phi_4)}\right\rangle\right\rangle \\
\langle\langle 6\rangle\rangle &\equiv \left\langle\left\langle e^{in(\phi_1+\phi_2+\phi_3-\phi_4-\phi_5-\phi_6)}\right\rangle\right\rangle \\
\langle\langle 8\rangle\rangle &\equiv \left\langle\left\langle e^{in(\phi_1+\phi_2+\phi_3+\phi_4-\phi_5-\phi_6-\phi_7-\phi_8)}\right\rangle\right\rangle
\end{aligned} \tag{4}$$

where ϕ_i is the azimuthal angle of the i-th particle, and $\langle\langle\rangle\rangle$ indicates that the average is taken over all m-particle combinations for all events. In order to remove self-correlations, it is required that the m particles be distinctive. The unbiased estimators of the reference m-particle cumulants, c_nm, are defined as

$$\begin{aligned}
c_n\{4\} &= \langle\langle 4\rangle\rangle - 2\cdot\langle\langle 2\rangle\rangle^2\,, \\
c_n\{6\} &= \langle\langle 6\rangle\rangle - 9\cdot\langle\langle 4\rangle\rangle\langle\langle 2\rangle\rangle + 12\cdot\langle\langle 2\rangle\rangle^3\,, \\
c_n\{8\} &= \langle\langle 8\rangle\rangle - 16\cdot\langle\langle 6\rangle\rangle\langle\langle 2\rangle\rangle - 18\cdot\langle\langle 4\rangle\rangle^2 + 144\cdot\langle\langle 4\rangle\rangle\langle\langle 2\rangle\rangle^2 - 144\langle\langle 2\rangle\rangle^4.
\end{aligned} \tag{5}$$

Correlating the m-particles within the reference phase space of $|\eta| < 2.4$ and p_T range of $0.3 < p_T < 3.0$ GeV/c, we then obtain the reference flow $v_2\{m\}$, with

$$\begin{aligned}
v_4\{4\} &= \sqrt[4]{-c_n4}\,, \\
v_6\{6\} &= \sqrt[6]{\frac{1}{4}c_n6}\,, \\
v_8\{8\} &= \sqrt[8]{-\frac{1}{33}c_n8}\,.
\end{aligned} \tag{6}$$

With respect to the reference flow, the differential $v_2m(p_T,\eta)$ can then be expressed as

$$v_2\{4\}(p_T,\eta) = -d_2\{4\}/\sqrt[3/4]{-c_n\{4\}}\,, \tag{7}$$

$$v_2\{6\}(p_T,\eta) = d_2\{6\}/\sqrt[5/6]{c_n\{6\}}/4^{1/6}\,, \tag{8}$$

$$v_2\{8\}(p_T,\eta) = -d_2\{8\}/\sqrt[7/8]{-c_n\{8\}}/33^{1/8}\,, \tag{9}$$

where the differential cumulants $d_2\{m\}$ are estimated by replacing one of the m-particle cumulants in Eq. (5) with a particle from a certain particle of interest (POI) phase space in p_T or η [17].

4 Results

The v_2 and v_3 results are shown in Figure 2. Those are measured by using the scalar product (SP) method as a function of p_T ($\approx$ 100 GeV/c) in 7 centrality ranges (0–60%) of PbPb collisions at $\sqrt{s_{\rm NN}}$ = 5.02 TeV. The statistical uncertainties are represented in the bars and the systematic uncertainties are denoted in the shaded boxes.

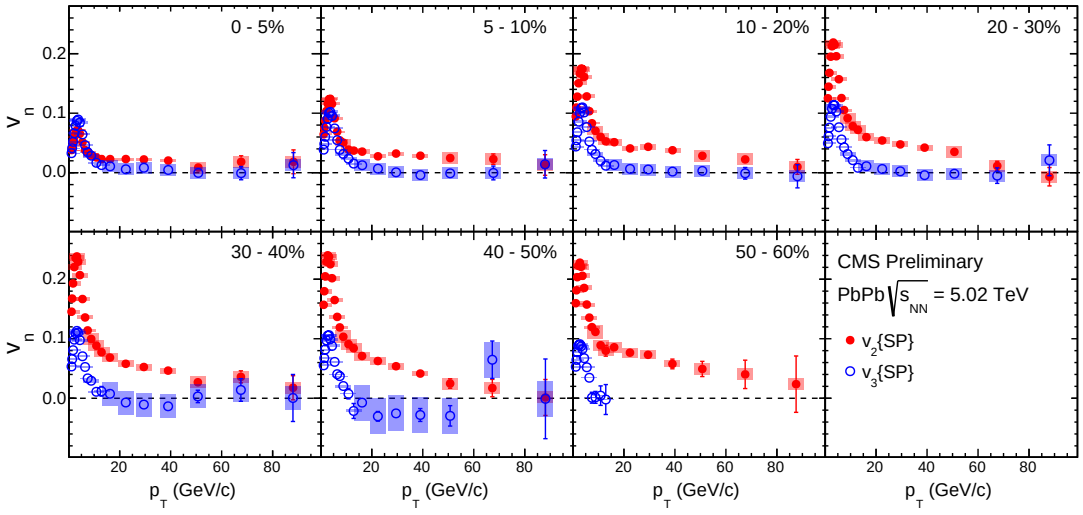

Figure 2. The v_2 and v_3 results from SP method as a function of p_T in seven centrality ranges of PbPb collisions at $\sqrt{s_{\rm NN}}$ = 5.02 TeV. Shaded boxes represent systematic uncertainties [17].

The significant positive v_2 values are observed in the most of centrality ranges up to $p_T \approx 100$ GeV/c. The v_2 value first rises and then falls off around 3 GeV/c quickly from low p_T to high p_T region. In the low p_T region, v_2 values are first increasing from most central to mid-peripheral events (30-40%), and then decreasing in the more peripheral centrality ranges. At the higher p_T region (>10 GeV/C), the v_2 values are slowly decreasing as p_T increases. The v_3 results show similar tendency as that for v_2. At low p_T, the observed v_3 values don't depend on centrality. Significant positive v_3 are found to continue up to p_T of 20 GeV/c for all centrality ranges. Above p_T= 20 GeV/c, the v_3 values are consistent with zero within given uncertainties. These results of v_2 and v_3 cover the widest p_T range ever achieved. Such a result at high p_T is sensitive to the path length dependence of hard partons in the QGP and will be expected to put more constrain on the energy loss models.

Figure 3 shows the comparison between v_2 results at $\sqrt{s_{\rm NN}}$ = 5.02 TeV and v_2 results obtained with the Event Plane (EP) at $\sqrt{s_{\rm NN}}$ = 2.76 TeV [20] and theoretical calculations from CUJET3.0 [21, 22] at 5.02 TeV. The results from SP and EP are similar up to very high p_T. The difference do not exceed 5%. The model (CUJET3.0) calculations are compatible with the results at high p_T(> 40 GeV/c) within systematic uncertainties in all over centrality ranges except for the most peripheral one where the model doesn't reproduce the data.

In order to investigate the origin of this correlation observed at very high p_T further, we obtained v_2 values from multi-particle cumulant analysis (4, 6 and 8) and compared with the SP v_2 results as shown in Figure 4. At low p_T (p_T < 3 GeV/c), the results follow the expectation from hydrodynamic models meaning $v_2\{\rm SP\} > v_2\{4\} \approx v_2\{6\} \approx v_2\{8\}$. At high p_T(10 GeV/c), scalar product and multi-particle correlation results tend to converge to the same value.

This observation suggests strong evidence that collective anisotropic particle emission in heavy ion collisions extend to very high p_T region. Although the nature of collectivity at high p_T is likely to be related to jet quenching phenomena, the observed anisotropies at both high and low p_T are related to initial-state geometry and its event-by-event fluctuations.

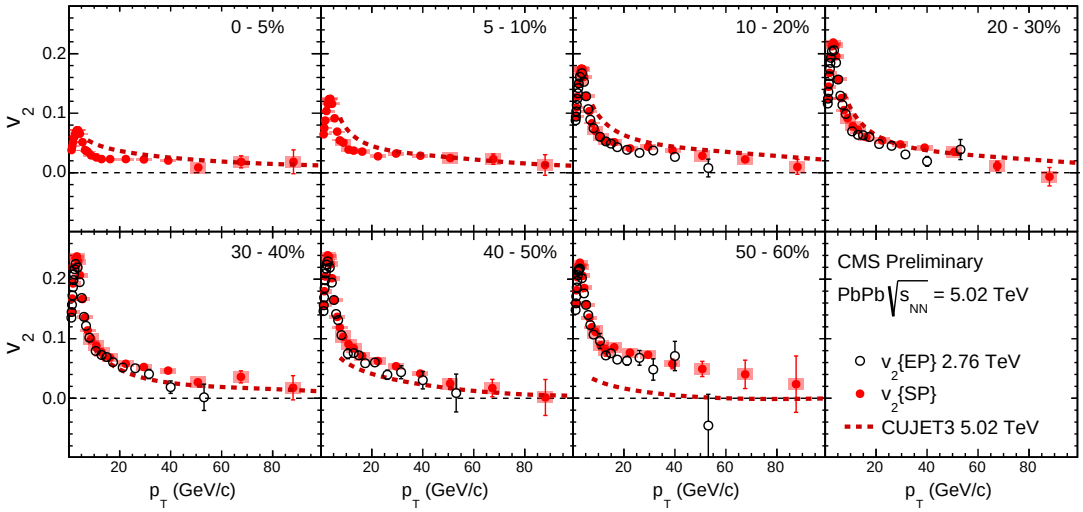

Figure 3. The v_2 results from SP and EP method as a function of p_T in seven centrality ranges of PbPb collisions at $\sqrt{s_{\rm NN}}$ = 5.02 TeV and 2.76 TeV respectively. Shaded boxes represent systematic uncertainties [17] and dashed lines are predictions from CUJET3.0 model [21, 22].

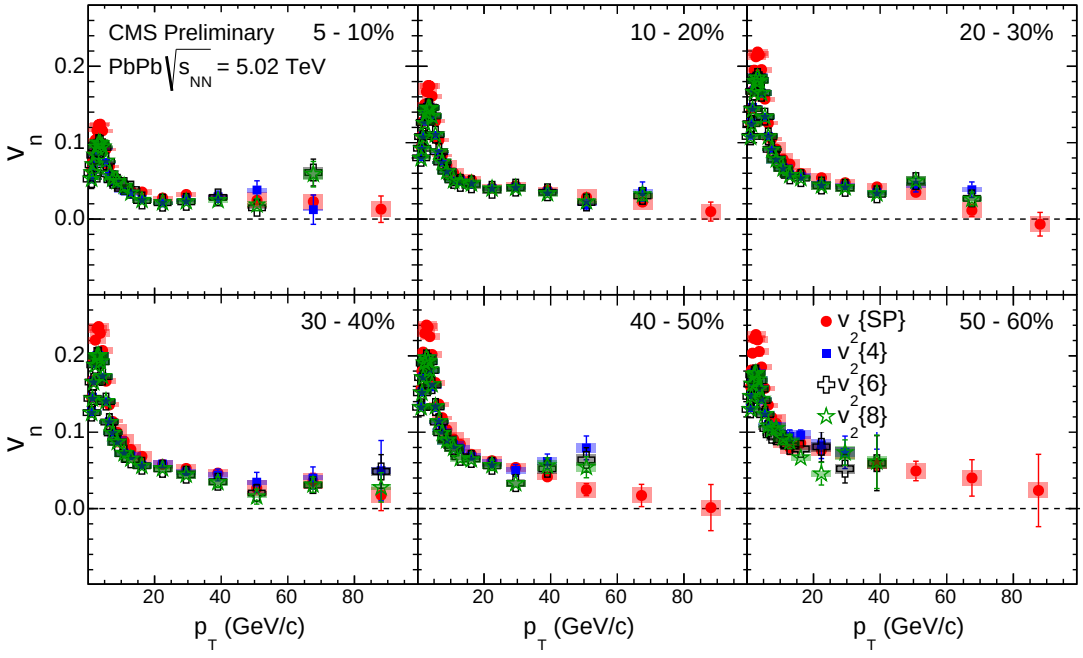

Figure 4. Comparison between the v_2 results from SP and cumulant methods as a function of p_T in six centrality ranges of PbPb collisions at $\sqrt{s_{\rm NN}}$ = 5.02 TeV. Shaded boxes represent systematic uncertainties [17].

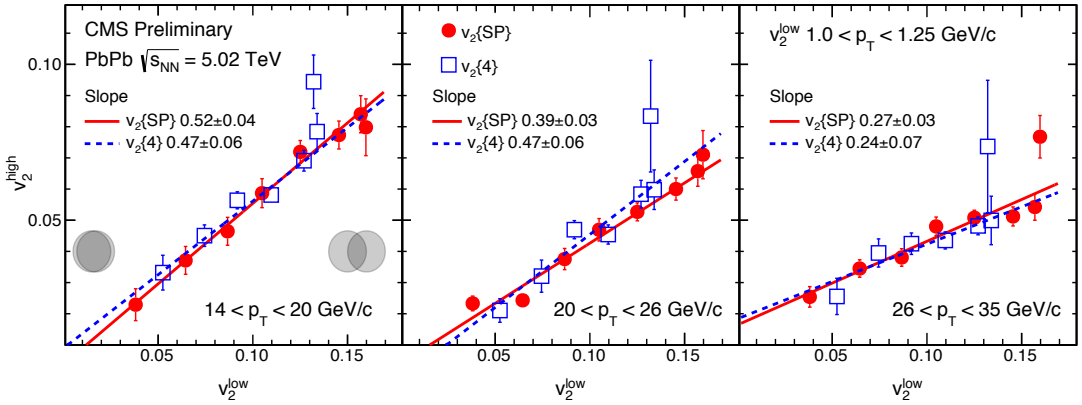

Figure 5. The v_2 values from different centrality ranges at high p_T : $12 < p_T < 14$ GeV/c, $20 < p_T < 26$ GeV/c and $26 < p_T < 35$ GeV/c vs. low p_T ($1 < p_T < 1.25$ GeV/c) obtained from SP (closed circles) and cumulant (open squares) methods in PbPb collisions at $\sqrt{s_{NN}}$ = 5.02 TeV [17].

To find possible connection of azimuthal anisotropies between low-p_T (dominated by hydrodynamics) and high p_T (dominated by jet quenching) regions, the correlation between the v_2 results at low and high p_T was studied. Figure 5 shows v_2 from $12 < p_T < 14$ GeV/c, $20 < p_T < 26$ GeV/c and $26 < p_T < 35$ GeV/c as a function of v_2 from $1.0 < p_T < 1.25$ GeV/c extracted from each centrality range of PbPb collisions at $\sqrt{s_{NN}}$ = 5.02 TeV. Each point represents a different centrality range starting from the most central events on the left toward peripheral events on the right. The first four points have a centrality bin width of 5% (from 0 to 20%) while, for the others, the bin width is 10%. Full circles are the results obtained from SP method and open square are extracted from 4-particle correlation analysis. A strong correlation of v_2 values between high and low p_T regions is observed over the full centrality range. While low p_T correlations can be explained by the collective expansion of the medium, high p_T correlations come from the path-length dependence of the hard-scattered partons undergo while traversing the medium. This indicates that the initial geometry and its fluctuations may be responsible for the correlations observed both at low and high p_T.

5 Summary

In summary, the azimuthal anisotropy of charged particles with respect to the event plane has been studied in PbPb collisions at $\sqrt{s_{NN}}$= 5.02 TeV using the CMS detector. The v_2 and v_3 values are measured over a wide p_T range from 1 GeV/c to 100 GeV/c in different collision centralities using scalar product method. The results cover for the first time the very high p_T region beyond 60 GeV/c. Moreover, these results provide a v_3 measurement up to a p_T region that has never before been studied (up to 100 GeV/c). The observed $v_2(p_T)$ shows a tendency of rapid increasing to a maximum at p_T of $\approx$ 3 GeV/c and a steep fall for all of centrality ranges. The $v_3(p_T)$ behavior is very similar to v_2 at low p_T but its value is consistent with zero over the full centrality range for $p_T > 20$ GeV/c. The observed trend in the centrality dependence of v_2 over a wide p_T range suggests a potential connection to the initial-state geometry. To further investigate the origin of the correlation at high p_T, a multi-particle correlation analysis was performed to extract v_2 from 1 GeV/c to, at maximum, 100 GeV/c. At low p_T, $v_2\{4\}$, $v_2\{6\}$ and $v_2\{8\}$ have similar values and smaller than $v_2\{\mathrm{SP}\}$. This follows hydrodynamic

expectations and is a sign of collectivity. The same behavior is observed at high p_T and reflects the collective nature of these correlations. As the last, the correlations between v_2 values at low and high p_T as a function of centrality have been studied. The results shows the strong correlations. The low and high p_T correlations are interpreted by the collective expansion and by the path-length dependence of hard-scattered partons in the medium, respectively. These results indicate that the initial geometry and its fluctuations are responsible for the low and high p_T correlations.

6 Acknowledgement

This paper was financially supported by Chonnam National University (Grant number: 2015-3039).

References

[1] BRAHMS Collaboration, Nucl. Phys. A **757**, 1 (2005)
[2] PHENIX Collaboration, Nucl. Phys. A **757**, 184 (2005)
[3] PHOBOS Collaboration, Nucl. Phys. A **757**, 28 (2005)
[4] STAR Collaboration, Nucl. Phys. A **757**, 102 (2005)
[5] Noronha-Hostler, Jacquelyn and Betz, Barbara and Noronha, Jorge and Gyulassy, Miklos, arXiv:1602.03788.
[6] Peigne, S. and Smilga, A. V., arXiv:0810.5702.
[7] Wicks, Simon and others, Nucl. Phys. A **784**, 426 (2007)
[8] Jia, Jiangyong and Wei, Rui, arXiv:1005.0645.
[9] Jia, Jiangyong and Horowitz, W.A. and Liao, Jinfeng, Phys. Rev. C **84**, 034904 (2011)
[10] Renk, Thorsten, Phys. Rev. C **83**, 024908 (2011)
[11] Betz, Barbara and Gyulassy, Miklos and Torrieri, Giorgio, Phys. Rev. C **84**, 024913 (2011)
[12] Betz, Barbara and Gyulassy, Miklos, arXiv:1201.0281.
[13] CMS Collaboration, https://twiki.cern.ch/twiki/bin/view/CMSPublic/HighLevelTriggerRunIIResults
[14] Poskanzer, Arthur M. and Voloshin, S. A., Phys.Rev. C **58**, 1671 (1998)
[15] Barrette, J. and others, Phys.Rev. C **56**, 3254-3264 (1997)
[16] Adler, C. and others, Phys.Rev. C **66**, 034904 (2002)
[17] CMS Collaboration, CMS PAS-HIN-15-014 (2015) http://cds.cern.ch/record/2156183?ln=en
[18] Bilandzic, Ante and Snellings, Raimond and Voloshin Sergei, Phys.Rev. C **83**, 044913 (2011)
[19] Bilandzic, Ante and Christensen, Christian Holm and Gulbrandsen, Kristjan and Hansen, Alexander and Zhou, You, Phys.Rev. C **89**, 064904 (2014)
[20] Chatrchyan, Serguei and others, Phys. Rev. Lett. **109**, 022301 (2012)
[21] Xu Jiechen and Liao Jinfeng and Miklos Gyulassy, Chinese Physics Letters **32**, 092501 (2015)
[22] Xu, Jiechen and Liao, Jinfeng and Gyulassy, Miklos, Journal of High Energy Physics **2016**, 1–50 (2016)